Simulation of Dendritic Solidification in Cubic and HCP Crystals by Cellular Automaton and Phase-Field Models

Mohsen Asle Zaeem*

(Ph.D., Assistant Research Professor)

Center for Advanced Vehicular Systems, Mississippi State University

Hebi Yin

(Ph.D., Postdoctoral Research Associate)

Oak Ridge National Laboratory

Sergio D. Felicelli

(Ph.D., Professor)

Mechanical Engineering Department, Mississippi State University

COMSOL CONFERENCE 2011

Motivation

Microstructures are the shape and alignment of the microscopic components of materials and may consist of:

- Spatially distributed phases of different compositions and/or crystal structures
- Grains of different orientations, domains of different structural variants
- Domains of different electrical or magnetic polarizations
- Structural defects

Microstructural evolution is common in many fields including biology, hydrodynamics, chemistry, and phase transformations.

Microstructures controls

- Mechanical
- Electrical
- Magnetic
- Optical
- Chemical

properties of materials

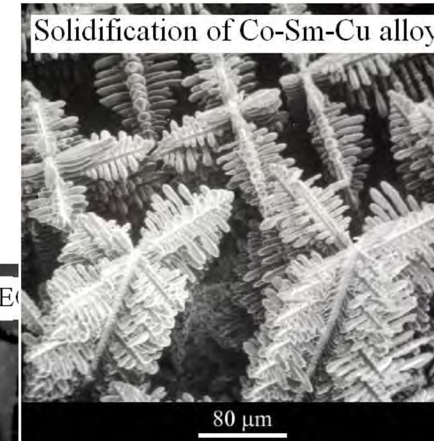

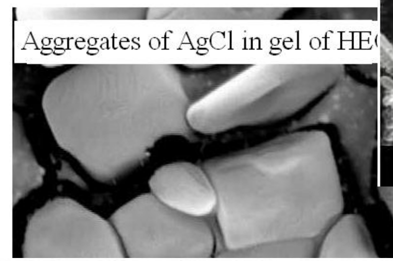

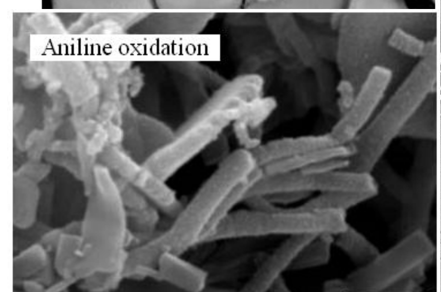

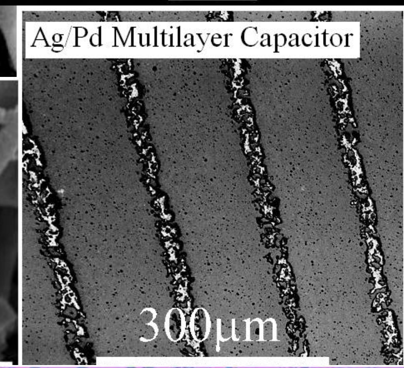

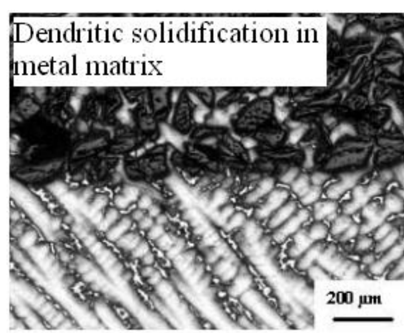

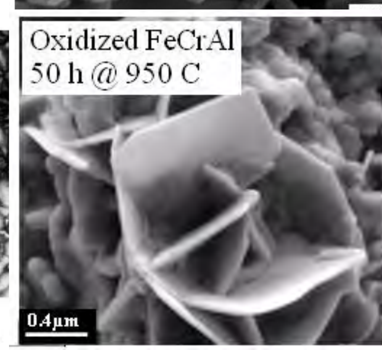

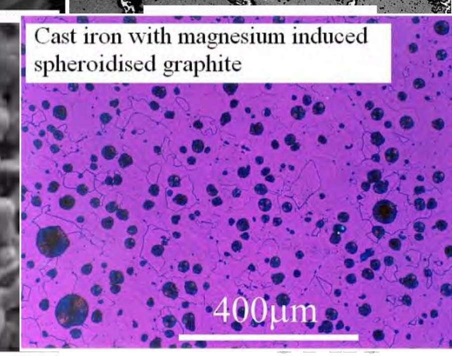

DoITPoMS, University of Cambridge, 2010.

Introduction

The study of free boundaries-interfacial regions can be grouped into two categories

Sharp-interface models

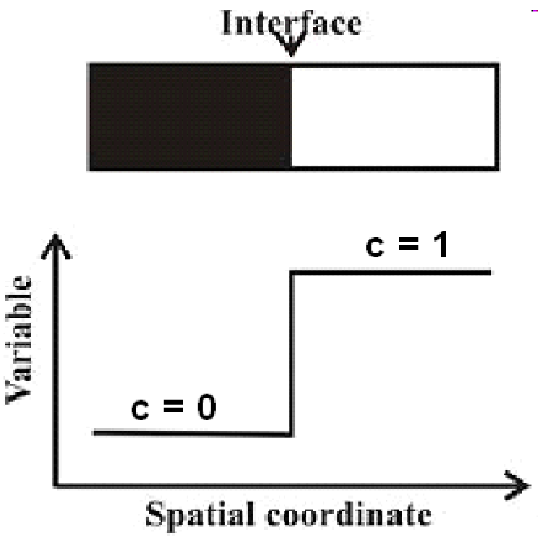

Phase-field models (diffusive interface)

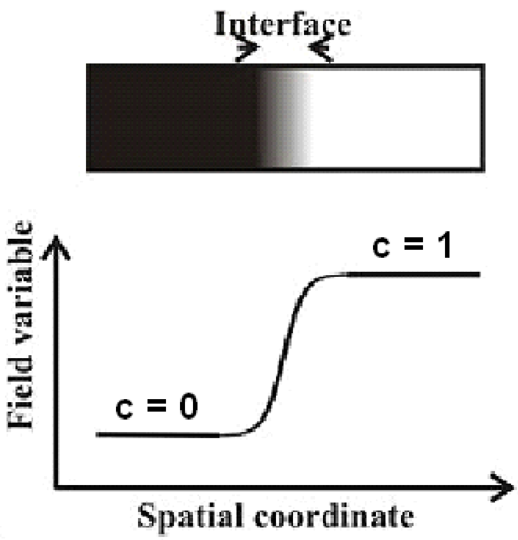

Non-conserved phase-field $\dot{\phi} = D_2(\phi)$

Solidification and melting

Conserved phase-field $\dot{\phi} = D_4(\phi)$

- Solid-state phase transformations (coupled to elasticity)
- Interfaces between immiscible fluids (coupled to Navier–Stokes)

L.-Q. Chen, Annu. Rev. Mater. Res. 32 (2002) 113.
G. Caginalp and W. Xie, Phys. Rev. E 48 (1993) 1897.

Introduction

Applications of Phase-Field Model

- Solid State Phase Transformation
- Phase Transformation in Thin Films
- Solidification
- Grain Growth polycrystalline materials
- Dislocation Dynamics
- Crack Propagation
- Electromigration
- Multi-Phase Fluid Flow
- .....

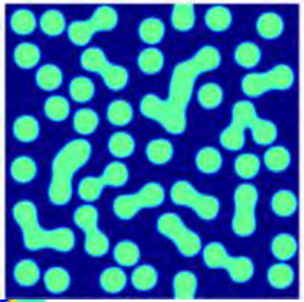
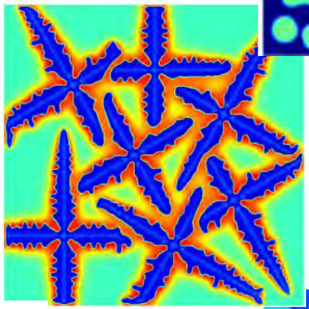
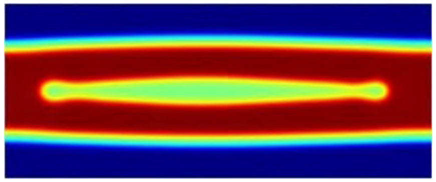
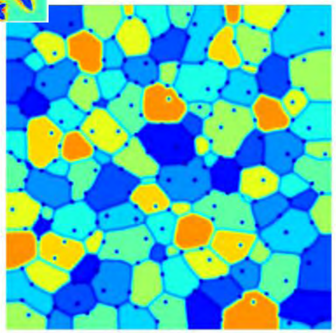
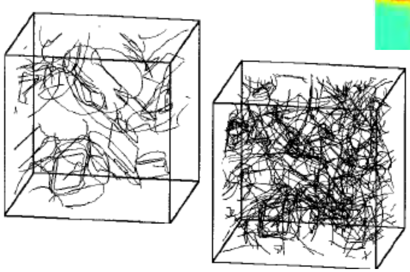
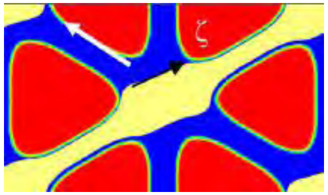

Long-Qing Chen, Phase-field models of microstructure evolution, Annu. Rev. Mater. Res. 32 (2002) 113-140.

Yunzhi Wang, Ju Li, Overview No. 150: Phase field modeling of defects and deformation, Acta Materialia 58 (2010) 1212–1235.

Introduction

Commonly Used Numerical Methods to Solve The Governing Equations of Phase-Field Models

- Finite difference method (FDM) (Cahn and Kobayashi 1995; Johnson 2000)

- Fourier-spectral methods (Chen and Shen 1998, 2009; Boisse et al. 2007)

<u>These methods have limitations in 2D and 3D models when irregular geometries or complex boundary conditions are involved</u>

We develop a general numerical method applicable to a variety of geometries and boundary conditions.

M. Asle Zaeem and S.Dj. Mesarovic, Journal of Computational Physics 229 (2010) 9135-9149.

Dendritic Solidification of Cubic and Hexagonal Materials

During solidification of metals and their alloys, the formation of complex dendrite microstructures has significant effects on the mechanical and material properties of cast alloys.

Dendritic Solidification of Cubic and Hexagonal Materials

Cellular automaton

Heat transfer: $\frac{\partial T}{\partial t} = \alpha \cdot \nabla^2 T + \frac{L}{\rho C_p}\frac{\partial f_s}{\partial t}$ (α → thermal diffusivity)

Mass transfer: $\frac{\partial C_i}{\partial t} = D_i \cdot \nabla^2 C_i + C_i \cdot (1-k)\frac{\partial f_s}{\partial t}$ (k → partition coefficient)

Solid/Liquid interface: $C_s = k \cdot C_l$

The increase solid fraction: $\Delta f_s = (C_l^* - C_l)/(C_l^* \cdot (1-k))$

Interface equilibrium composition:

$$C_l^* = C_0 + \frac{T^* - T_l^{eq} + \Gamma K f(\varphi, \theta_0)}{m_l}$$

- T_l^{eq} → equilibrium liquidus T at C_0
- Γ → Gibbs-Thomson coefficient
- K → curvature at SL interface
- T^* → interface equilibrium T
- m_l → liquidus slope

Function of anisotropy of surface tension:

$$f(\varphi, \theta_0) = 1 - \delta \cos[4(\varphi - \theta_0)]$$

- θ_0 → preferential direction
- φ → growth angle
- δ → anisotropy coefficient

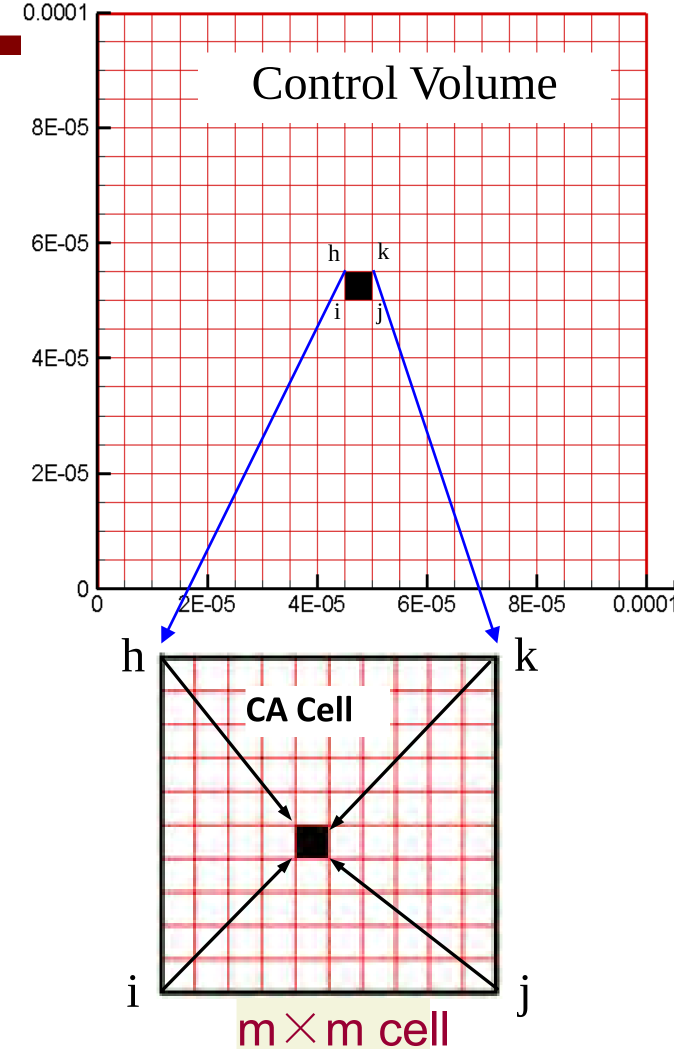

Time step for mass: $\Delta t_C = \frac{\Delta x^2}{4.5 D_l}$

Time step for heat: $\Delta t_T = \frac{\rho C_p (m \cdot \Delta x)^2}{4.5\lambda}$ (Δx → cell size)

Ration of two time steps: $N_t = \Delta t_C / \Delta t_T$

Dendritic Solidification of Cubic and Hexagonal Materials

COMSOL CONFERENCE 2011

Cellular automaton (Pb-23%Sn)

Pb, cubic structure with four-fold symmetry

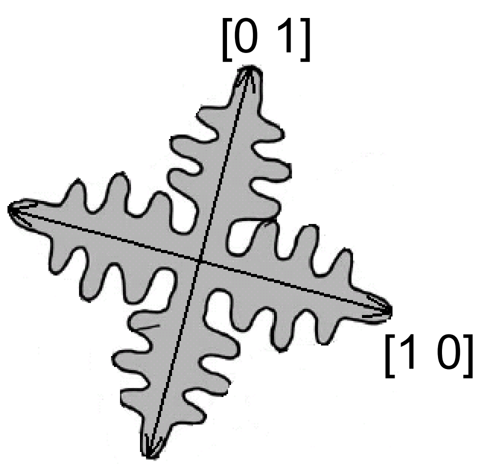

Low cooling rate

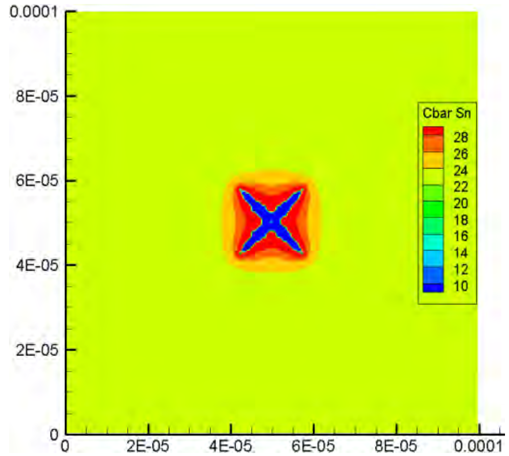

Low cooling rate

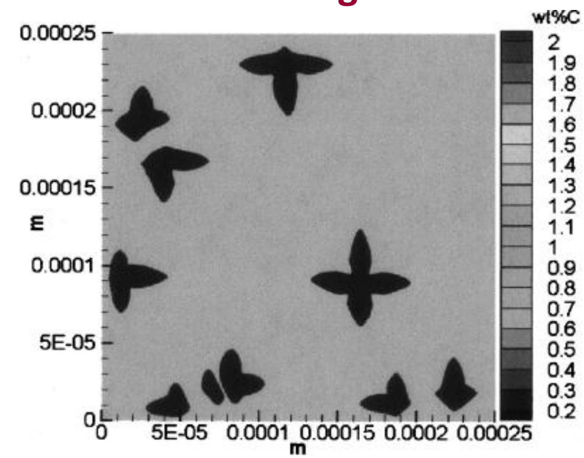

High cooling rate

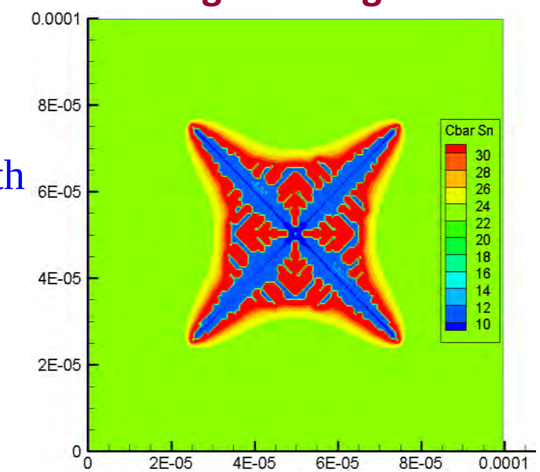

High cooling rate

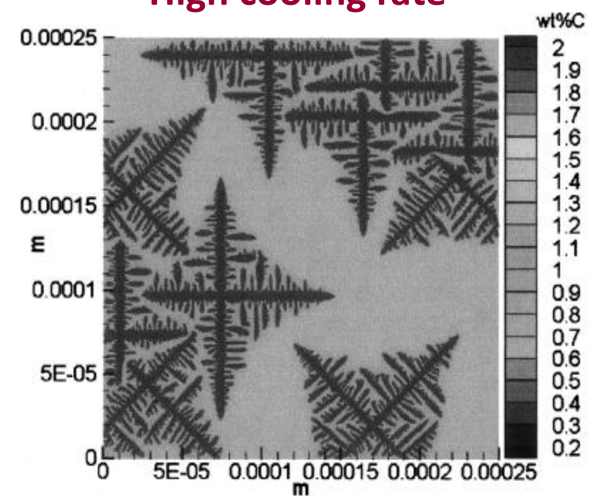

Stefanescu et al, 2003

- Dendrite morphology at 0.1 s with different cooling rates caused by different BCs, and comparison to published results
- Higher cooling rate enhances the formation of secondary arm

Dendritic Solidification of Cubic and Hexagonal Materials

Cellular automaton

HCP crystal structure with six-fold symmetry

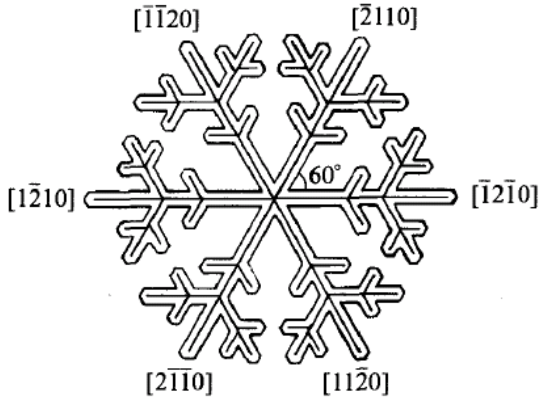

(0001) basal plane

? Problem of result: The angle between the primary arms is not 60 degree. It grows aligning with the axis of the mesh, or at 45 degree

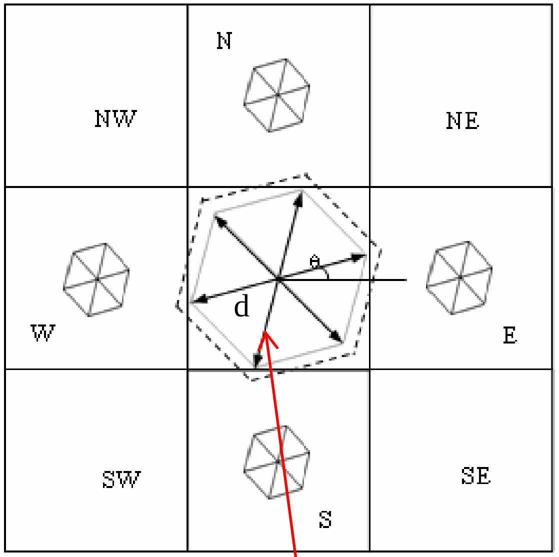

Growth in six directions

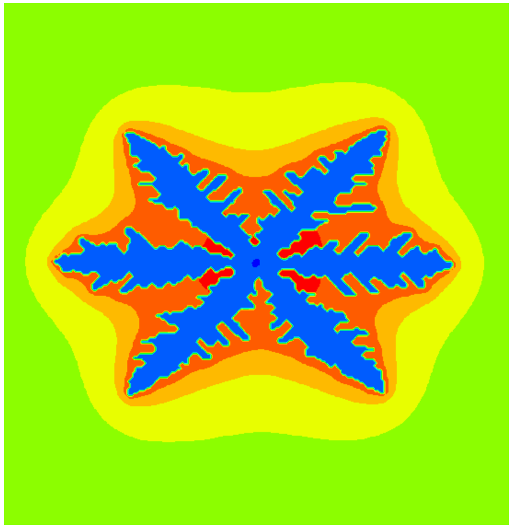

Map of composition

Cellular automaton

- CA – grid dependent anisotropy, (*Krane , et al. 2008*)
- Hexagonal mesh reduces grid-induced anisotropy, (*Grest, et al. 1985*)

2D hexagonal mesh is generated to simulate the HCP crystal material

FE Mesh

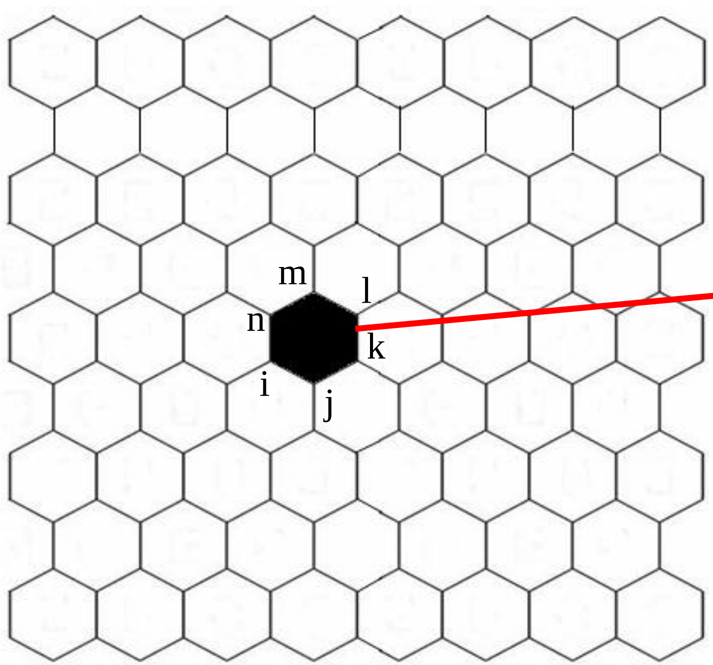

Hexagonal mesh for heat transfer

CA Cell

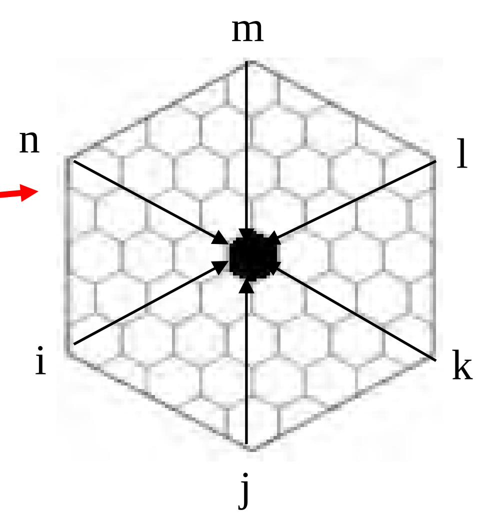

Mass transfer and dendrite growth

Phase-field model

Kobayashi's Model –Pure Materials

(R. Kobayashi, Physica D 63 (1993) 410-423)

$$F(\phi,m)=\int_V \left(f_{local}(\phi,m)+f_{grad}(\phi)\right)dV$$

$$f_{local}(\phi,m)=\int_0^{\phi}\phi(\phi-1)(\phi-\frac{1}{2}+m)d\phi$$

$$f_{grad}(\phi)=\kappa^2(\nabla\phi)^2/2$$

$$\alpha(\theta)=\bar{\alpha}\sigma(\theta)$$

$$m(T)=(\alpha/\pi)\tan^{-1}[\gamma(T_e-T)]$$

$$\sigma(\theta)=1+\delta\cos[j(\theta-\theta_0)]$$

$$\theta=\tan^{-1}\left(\frac{\partial\phi/\partial y}{\partial\phi/\partial x}\right)$$

$$\varepsilon\frac{\partial\phi}{\partial t}=-\frac{\delta F}{\delta\phi}$$

Time-dependent Ginzburg-Landau (TDGL) equation

$$\varepsilon\frac{\partial\phi}{\partial t}=-\frac{\partial}{\partial x}\left(\alpha\alpha'\frac{\partial\phi}{\partial y}\right)+\frac{\partial}{\partial y}\left(\alpha\alpha'\frac{\partial\phi}{\partial x}\right)+\nabla\cdot(\alpha^2\nabla\phi)+\phi(1-\phi)(\phi-\frac{1}{2}+m)$$

$$\frac{\partial T}{\partial t}=\nabla^2T+K\frac{\partial\phi}{\partial t}$$

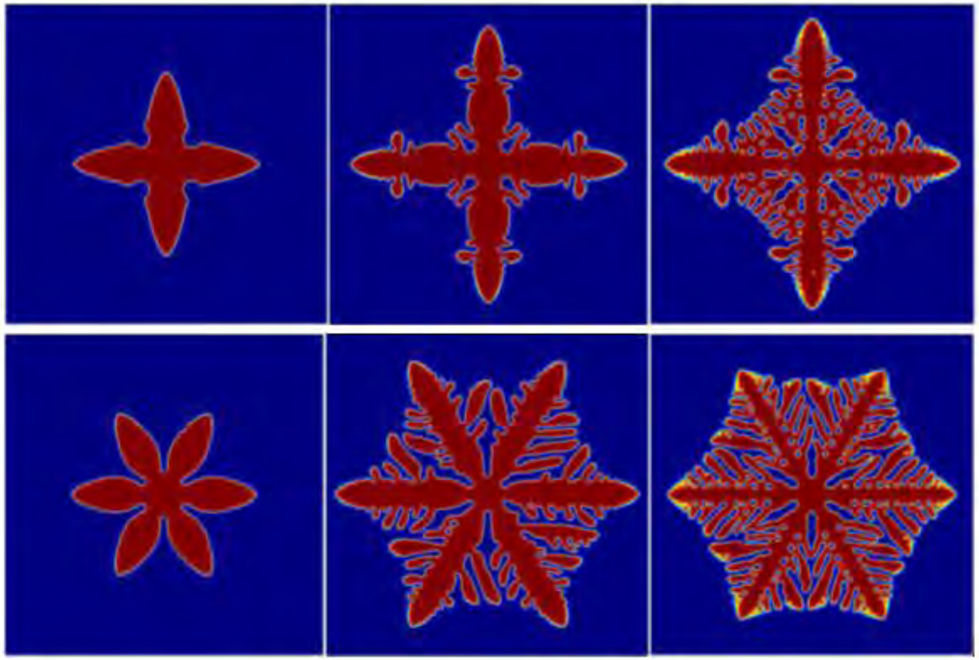

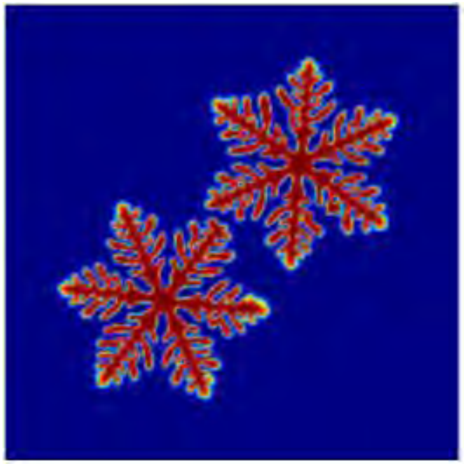

For a binary alloy, the Gibbs-Thomson equation for an isotropic surface energy can be written as

$$\frac{1}{\mu|\nabla\phi|}\frac{\partial\phi}{\partial t} = T_m - T + m_l C_l - \Gamma\nabla\cdot\mathbf{n} \qquad \mathbf{n} = -\frac{\nabla\phi}{|\nabla\phi|}$$

Diffusion coef.

$$\tilde{D} = D_s + (D_l - D_s)\frac{1-\phi}{1-\phi+k\phi}$$

Density

$$\tilde{\rho} = \rho_s + (\rho_l - \rho_s)\frac{1-\phi}{1-\phi+k\phi}$$

(I) $$\frac{\partial C}{\partial t} = \nabla\cdot\tilde{D}\left[\nabla C - \frac{(1-k)C)}{1-\phi+k\phi}\nabla\phi\right]$$

(II) $$\frac{\partial T}{\partial t} = k\cdot\nabla^2 T + \frac{L}{\tilde{\rho}C_{\mathrm{P}}}\frac{\partial\phi}{\partial t}$$

(III) $$\frac{\partial\phi}{\partial t} = \mu\Gamma\left[-\frac{\partial}{\partial x}\left(\alpha\alpha'\frac{\partial\phi}{\partial y}\right) + \frac{\partial}{\partial y}\left(\alpha\alpha'\frac{\partial\phi}{\partial x}\right) + \nabla\cdot(\alpha^2\nabla\phi) - \frac{\phi(1-\phi)(1-2\phi)}{\lambda^2}\right] + \mu(T_m - T + m_l C_l)\frac{\phi(1-\phi)}{\lambda}$$

Governing Equations Solved by Math Module COMSOL multiphysics

COMSOL CONFERENCE 2011

Properties of Al-3.0 wt.% Cu alloy

Property	*Value*
Thermal expansion coefficient (β_T)	-2.6×10^{-5} K^{-1}
Density	2475 kg m^{-3}
Diffusivity of alloy elements in liquid (D_l)	3.0×10^{-9} m^2 s^{-1}
Diffusivity of alloy elements in solid (D_S)	3.0×10^{-13} m^2 s^{-1}
Thermal conductivity	30 J K^{-1} m^{-1} s^{-1}
Average specific heat	500 J kg^{-1} K^{-1}
Latent heat of fusion (L)	3.76×10^4 J kg^{-1}
Gibbs-Thomson coefficient	2.4×10^{-7} K·m
Liquidus slope	-2.6 K/wt pct
Partition ratio	0.17
Melting temperature of pure substance	933.6 K

Dendritic Solidification of Cubic Materials

Cellular automaton versus Phase-field model

Al–3.0 wt.% Cu alloy

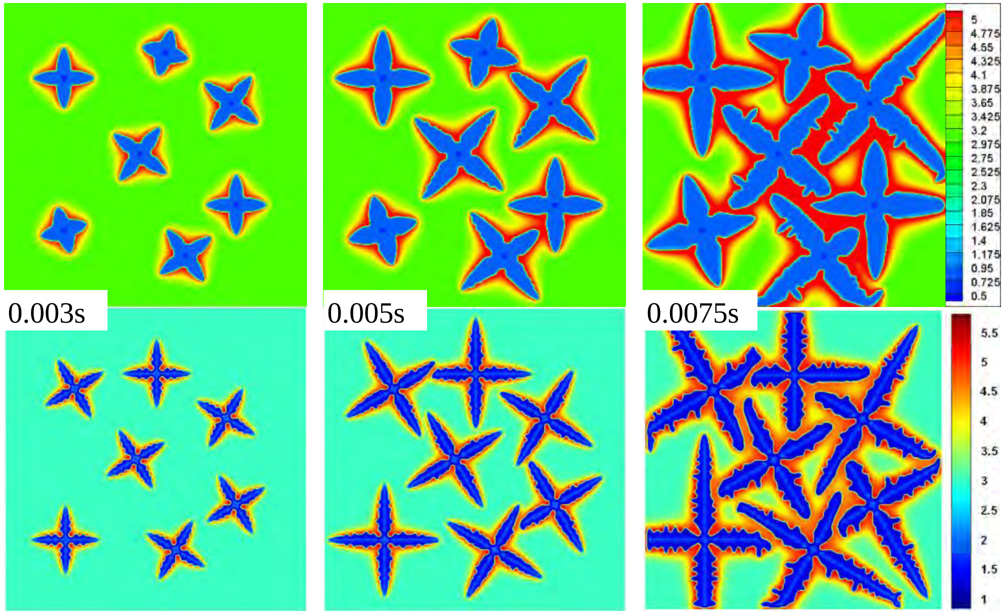

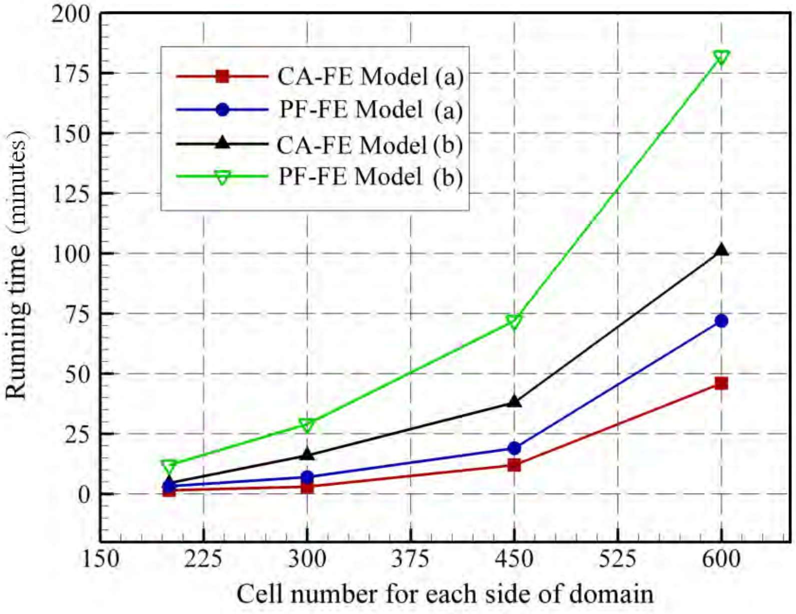

Cellular automaton versus Phase-field model

Al–3.0 wt.% Cu alloy

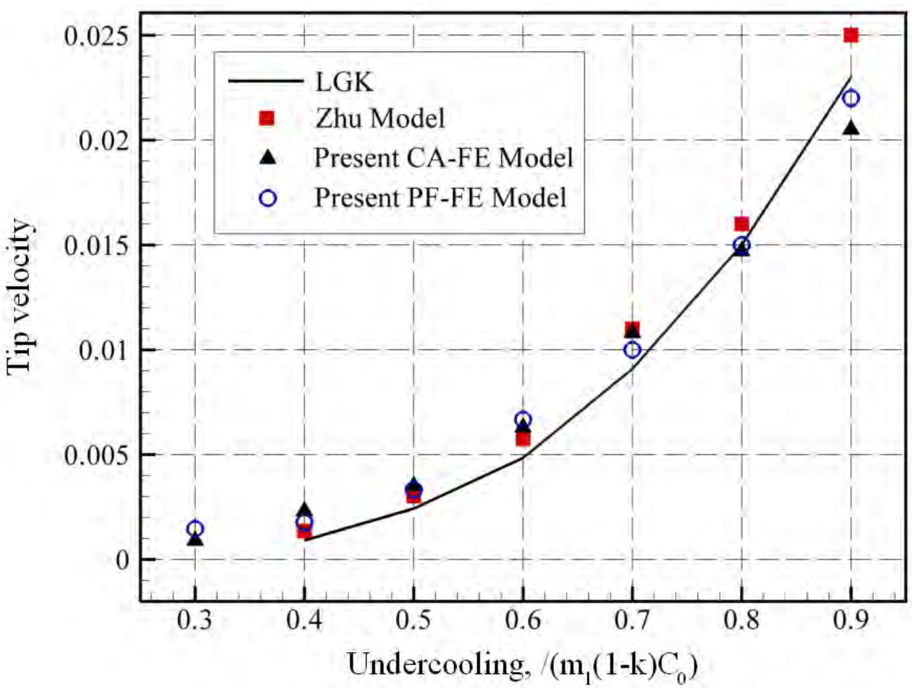

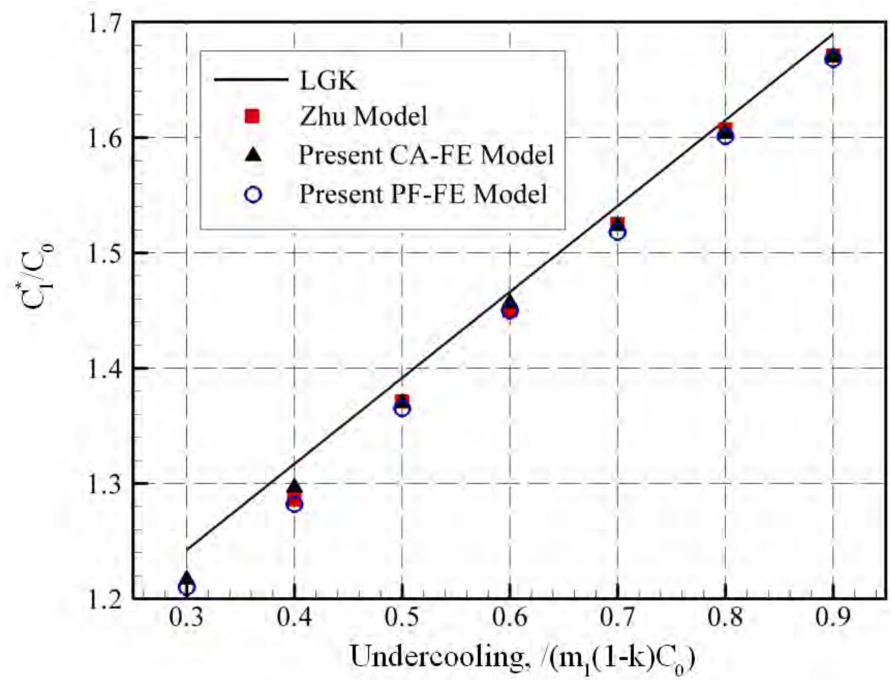

MgAZ91 alloy properties

Property	*Value*
Thermal expansion coefficient (β_T)	-2.6×10^{-5} K^{-1}
Density of liquid (ρ_l) Density of solid (ρ_s)	1650 kg m^{-3} 1750 kg m^{-3}
Viscosity (μ)	2×10^{-3} N s m^{-2}
Diffusivity of alloy elements in liquid (D_l) Diffusivity of alloy elements in solid (D_s)	5.0×10^{-9} m^2 s^{-1} 5.0×10^{-13} m^2 s^{-1}
Thermal conductivity in liquid (λ_l) Thermal conductivity in solid (λ_s)	80 J K^{-1} m^{-1} s^{-1} 105 J K^{-1} m^{-1} s^{-1}
Average specific heat of liquid (c_l) Average specific heat of solid (c_s)	1350 J kg^{-1} K^{-1} 1200 J kg^{-1} K^{-1}
Latent heat of fusion (L)	3.7×10^{5} J kg^{-1}
Liquidus temperature (T_R)	868 K
Eutectic temperature (T_E)	705 K
Gibbs-Thomson coefficient	2.0×10^{-7} K·m

Dendritic Solidification of Hexagonal Materials

Developed Phase-Field Models using COMSOL

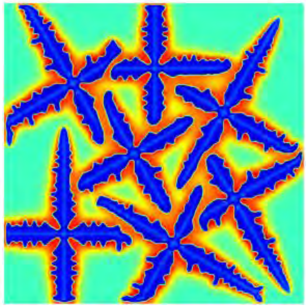

- **Dendritic Solidification of Cubic and Hexagonal Lightweight Materials**
  - Significance: - **multi-component alloys solidification was developed**
    - **multiple-arbitrary orientated hexagonal dendrites**

  M. Asle Zaeem et al., Mater. Manuf. Processes (2011).

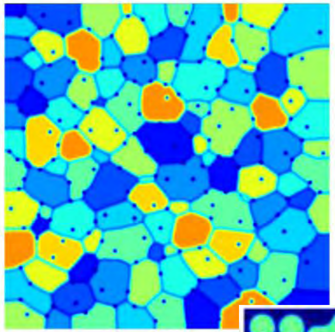

- **Grain Growth in Polycrystalline Materials**
  - Significance: **anisotropic grain boundary energy incorporated in phase-field model**

  M. Asle Zaeem et al., Comput. Mater. Sci. 50 (8) (2011) 2488-2492.

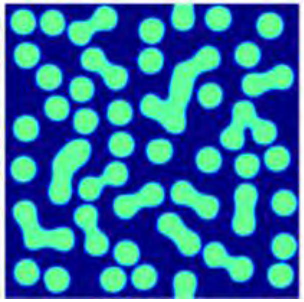

- **Phase transformation in binary alloys**
  - Significance: **maps of transformations of binary multilayers**

  M. Asle Zaeem et al., J. Phase Equilib. Diff. 32 (2011) 302-308.

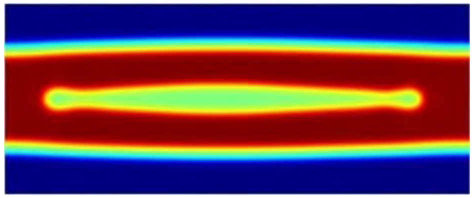

- **Morphological Instabilities in Multilayers**
  - Significance: **maps of transformations of binary multilayers**

  M. Asle Zaeem & S. Mesarovic , Comput. Mater. Sci. 50 (3) (2011) 1030-1036.

  M. Asle Zaeem et al., Modern Physics Letters B 25 (2011) 1591-1601.

- **Oxidation of Zirconium Alloys in Nuclear Power Plants**
  - Significance: **kinetics of oxidation was captured**

  M. Asle Zaeem et al., J. Nuclear Mater. (2011)-submitted

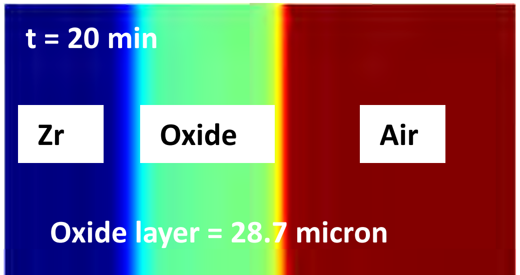

Mississippi State University

James Worth Bagley College of Engineering, Mississippi State University

CAVS

Future Research

➢ **3D phase-field finite-element modeling of solidification**

➢ **Study the effects of adding new elements on dendrite shape and spacing (alloys design)**

➢ **Interaction between bifilms and dendrites: oxide bifilms initiate defects after casting**

➢ **Study crystallization of polymers**

Questions?

Thank you!